

# Towards Robust SDRTV-to-HDRTV via Dual Inverse Degradation Network

Kepeng Xu<sup>1,2</sup> Gang He<sup>1,3\*</sup> Li Xu<sup>1</sup> Xingchao Yang<sup>2</sup> Ming Sun<sup>3</sup>  
Yuzhi Wang<sup>2</sup> Zijia Ma<sup>1</sup> Haoqiang Fan<sup>2</sup> Xing Wen<sup>3</sup>  
<sup>1</sup> Xidian University <sup>2</sup> Megvii Technology <sup>3</sup>Kuaishou Technology

kepengxu11@gmail.com ghe@xidian.edu.cn

## Abstract

Recently, the transformation of standard dynamic range TV (SDRTV) to high dynamic range TV (HDRTV) is in high demand due to the scarcity of HDRTV content. However, the conversion of SDRTV to HDRTV often amplifies the existing coding artifacts in SDRTV which deteriorate the visual quality of the output. In this study, we propose a dual inverse degradation SDRTV-to-HDRTV network DID-Net to address the issue of coding artifact restoration in converted HDRTV, which has not been previously studied. Specifically, we propose a temporal-spatial feature alignment module and dual modulation convolution to remove coding artifacts and enhance color restoration ability. Furthermore, a wavelet attention module is proposed to improve SDRTV features in the frequency domain. An auxiliary loss is introduced to decouple the learning process for effectively restoring from dual degradation. The proposed method outperforms the current state-of-the-art method in terms of quantitative results, visual quality, and inference times, thus enhancing the performance of the SDRTV-to-HDRTV method in real-world scenarios.

## 1. Introduction

High dynamic range television (HDRTV) has become increasingly popular because it can more realistically reproduce real-world luminance and color information, providing people with a better video viewing experience. The main differences between SDRTV and HDRTV are dynamic range, color gamut, and bit depth. However, despite the advances in HDRTV technology, there is a lack of available HDRTV content. Therefore, the conversion of SDRTV to HDRTV is an important work as it can help to alleviate the scarcity of HDRTV content and improve the video viewing experience for consumers.

Convolutional neural networks are well suited for low-level image and video enhancement. At this stage, there have been a large number of specific applications, such as video restoration[5, 7], image restoration[6, 17], im-

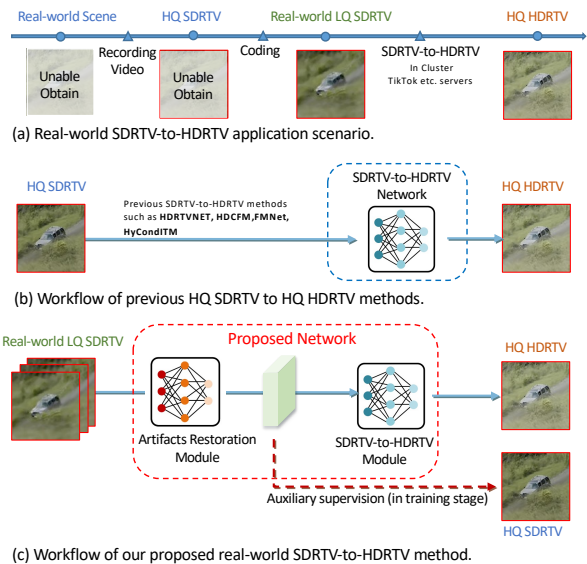


Figure 1. (a) Real-world SDRTV-to-HDRTV application scenario. Due to distribution copyright and historical technical limitations, usually media distribution companies do not have high-quality (HQ) SDRTV (nearly lossless), but only have relatively low-quality (LQ) version. (b) Workflow of previous HQ SDRTV to HQ HDRTV methods. Previous methods were able to convert HQ SDRTV to HQ HDRTV, but inputting LQ SDRTV using these methods in real world amplifies encoding artifacts. (c) Workflow of our proposed real-world SDRTV-to-HDRTV method. For converting real-world LQ SDRTV to HQ HDRTV, we propose a dual inverse degradation restoration network.

age denoising[35], and image synthesis[31, 32], and so on. Therefore, the convolutional neural network based method has emerged to convert SDRTV to HDRTV. The existing methods [3, 8, 27, 21] can effectively convert SDRTV to HDRTV frame by frame through feature modulation and dynamic convolution.

We combined the actual needs of SDRTV-to-HDRTV with the existing technology for analysis and got three observations.

The first observation is that the frame-by-frame SDRTV-



Figure 2. Artifacts in converted HDRTV. In methods such as HDCFM[8], the luminance range becomes larger, which will amplify the slight amount of artifacts present in SDRTV, resulting in severe artifacts in the output HDRTV. Our method aims to remove noise and artifacts and shows promising results on visual quality.

to-HDRTV method extracts the current frame information for feature modulation, and ignores the multi-frame information for color restoration. The single-frame method is prone to the discontinuity between frames.

The second observation is that solving the issue of the coding artifacts being amplified during the inverse tone mapping process is indispensable. Due to some historical technical and copyright reasons, a large number of current SDRTV videos do not have approximately lossless versions, and only relatively low-quality SDRTVs exist. Therefore, the SDRTV-to-HDRTV method needs to convert low-quality (LQ) SDRTV to high-quality (HQ) HDRTV in practical applications, as shown in Figure 1 (a). Meanwhile, previous works [28, 1] found that the conventional method of converting LQ SDRTV to HDRTV amplifies the coding artifacts. As shown in Figure 2, LQ SDRTV with inverse tone mapping exhibits significant coding artifacts.

In particular, we found that compared to SDRTV, HDRTV has more information in the high-frequency domain (third observation), so enhancing features in the frequency domain can effectively improve the quality of HDRTV.

According to the above three observations, we model practical SDRTV-to-HDRTV as a dual inverse degradation task (video restoration and inverse tone mapping). Previous methods convert high-quality SDRTV to high-quality HDRTV, as shown in Fig.1(b). But usually SDRTV is not of high quality in real scenes, and this gap will lead to poor performance of such methods.

In our DIDNet, temporal-spatial feature alignment and auxiliary loss are proposed to improve the spatial texture quality of HDRTV. Furthermore, to improve color restoration quality, a dual modulation convolution that cooperates with a 3D ConditionNet has been designed. Finally, we propose a wavelet attention module to enhance the frequency domain features to further improve the HDRTV quality. The proposed DIDNet (Fig. 1 (c)) is able to perform dual degradation recovery simultaneously, making the SDRTV-to-HDRTV method really move towards real applications.

Our contributions include four main points.

- We investigate that the HDRTV obtained by SDRTV-to-HDRTV conversion in real application scenarios has the problem of excessive amplification of coding artifacts. For the first time, a multi-reference frame alignment method is proposed to solve the serious problem of HDRTV artifacts.
- We reveal inverse tone mapping and artifact restoration are coupled in the process of SDRTV-to-HDRTV. Therefore, an auxiliary loss is designed to learn artifact removal, which allows efficient learning of dual restorations using a single end-to-end network.
- We analyze the computational mode of feature modulation and design a lighter and more efficient double modulation convolution.
- We discovered that HDRTV has more high-frequency information, so we proposed wavelet attention to improve the quality of HDRTV in the frequency domain.

## 2. Related work

SDRTV-to-HDRTV conversion is the reconstruction of standard dynamic range video (SDRTV) images into high dynamic range video (HDRTV). [13, 15] first studied the problem of super-resolution and SDRTV-to-HDRTV together. In these works, the input image is decomposed into a detail component for texture reconstruction and a base component for contrast enhancement. Specifically, [15] first performs the SDRTV-to-HDRTV conversion using a convolutional neural network (CNN). Then, [13] introduces modulation blocks to modulate the local intensity in a spatially varying manner to achieve adaptive local contrast enhancement. Recently, [3] has proposed a scheme for SDRTV-to-HDRTV. Inspired by the SDR/HDR formation process, [3] proposes a three-step solution pipeline that includes adaptive global color mapping, local enhancement, and highlight generation. [3] also provides a benchmark dataset called HDRTV1K for SDRTV to HDRTV conversion. [8, 21] proposes a model for joint local and global feature modulation[11, 26, 12] capable of local adaptive tuning. [8] proposes a feature mapping model and uses dynamic convolution to model feature transformations, thus completing the inverse tone mapping process more accurately. [27] uses the discrete cosine transform to enhance the low frequency information, which is used to reduce artifacts in the low frequency part.

Although these methods successfully perform inverse tone mapping, the existing SDRTV always has some degradation (coding artifacts). These degradations are amplified during the inverse tone mapping process, resulting in poor quality HDRTV from the conversion. Unlike the previous methods, this paper addresses the above encoding degradation recovery problem and designs a lighter and more accurate solution.

rate dual modulation convolution for more accurate inverse tone mapping.

### 3. Methodology

This section details the motivations and solutions in the SDRTV-to-HDRTV process.

#### 3.1. Motivations

**Artifacts in generated HDRTV.** Typically, video content undergoes a video coding process to reduce storage costs, which results in some artifacts during video coding. The extent of artifact distortion is determined by the bit rate utilized for encoding and the complexity of the scene. In most cases, SDRTV is encoded with an 8-bit depth, leading to the presence of encoding artifacts. As mentioned in [28, 1], these artifacts are amplified during the inverse tone mapping process. If the coding artifacts are not adequately addressed, the visual quality of the resulting HDRTV output will be poor.

**Limitations of single-frame global feature modulation (GFM).** Previous methods only perform inverse tone mapping in the form of single-frame global feature modulation. Specifically, a state vector is predicted by the image of the current frame, and then global broadcast multiplication and addition is performed on the state vector and the image features extracted from the current frame. This single-frame adaptive processing is hindered by the lack of continuity between frames. Additionally, the computational complexity of feature modulation increases as the video frame resolution increases.

**Dual degradation learning.** Previous methods only restore from single degradation (tone mapping), but in real-world applications, coding artifacts can lead to the unacceptable visual quality of HDRTV generated by these methods. SDRTV-to-HDRTV is a dual inverse degradation learning process, i.e., the restoration for coding artifacts and inverse tone mapping. This complexity makes it challenging to learn dual degeneration using a single model. A straightforward solution is to employ two separate models where the first model trains only for restoration and the second model learns only inverse tone mapping. However, successive independent training of such multiple submodels leads to cumulative errors and performance degradation due to poor coordination. To address this issue, we propose an auxiliary loss to facilitate coupled learning of dual degradation.

**Less high frequency information in SDRTV.** During our research, we found that HDRTV contains richer high-frequency information compared to SDRTV, as shown in Figure 4. Consequently, enhancing the feature in frequency domain can improve the visual quality of HDRTV.

#### 3.2. Overall of dual inverse degradation network

As elaborated by us previously, we propose the dual inverse degradation model to address the issue of coding artifact restoration in converted HDRTV, which allows for efficient learning of dual recovery using a single end-to-end model. The overall framework is presented in Fig.3.

First, the low-quality SDRTV frame  $X_{LS}$  is input to the temporal-spatial alignment feature fusion module  $TSAF$  to obtain  $F_{fusion}$ .

$$F_{fusion} = TSAF(X_{LS}) \quad (1)$$

The predicted high-quality SDRTV frames  $\ddot{X}_{HS}$  are obtained by convolving  $F_{fusion}$  with a  $3 \times 3$  convolution.

$$\ddot{X}_{HS} = Conv_{3 \times 3}(F_{fusion}) \quad (2)$$

Auxiliary loss  $L_{Aux}$  is computed using  $\ddot{X}_{HS}$  with high-quality SDRTV frames  $X_{HS}$ , thus allowing  $TSAF$  to learn the coding artifact inverse degradation process in a targeted manner.

$$L_{Aux} = L_1(\ddot{X}_{HS}, X_{HS}) \quad (3)$$

Meanwhile,  $F_{fusion}$  and  $X_{LS}$  are input to the dual-modulated convolution module  $DMC$  to obtain the modulated feature  $F_{Modulated}$ .

$$F_{Modulated} = DMC(F_{fusion}, X_{LS}) \quad (4)$$

The  $F_{Modulated}$  is input to the wavelet attention module  $WA$  to enhance the feature in the frequency domain, then a  $3 \times 3$  convolution is performed to obtain the predicted high-quality HDRTV frame  $\ddot{X}_{HH}$ , and the main loss  $L_{Main}$  is calculated with the high-quality HDRTV frame  $X_{HH}$ . Both loss functions use  $L_1$ .

$$\begin{aligned} \ddot{X}_{HH} &= Conv_{3 \times 3}(WA(F_{Modulated})) \\ L_{Main} &= L_1(\ddot{X}_{HH}, X_{HH}) \end{aligned} \quad (5)$$

#### 3.3. Restoration: temporal-spatial alignment quality enhancement

To leverage the temporal information while overcoming artifacts, we propose a temporal-spatial alignment method based on deformable convolution [4, 25, 34]. The input SDRTV frame  $X_{LS}$  is first processed by predicting the offset  $F_{offset}$  with an Unet-like structure. Subsequently, deformable convolution is performed using  $F_{offset}$  to obtain spatially aligned features  $F_{Aligned}$ . These aligned features are then further enhanced by aggregating them using residual blocks to obtain the fused features  $F_{fusion}$ .

#### 3.4. Auxiliary Supervision: restoring high quality SDRTV

In the motivation, it was mentioned that learning coding artifact recovery and inverse tone mapping simultaneously

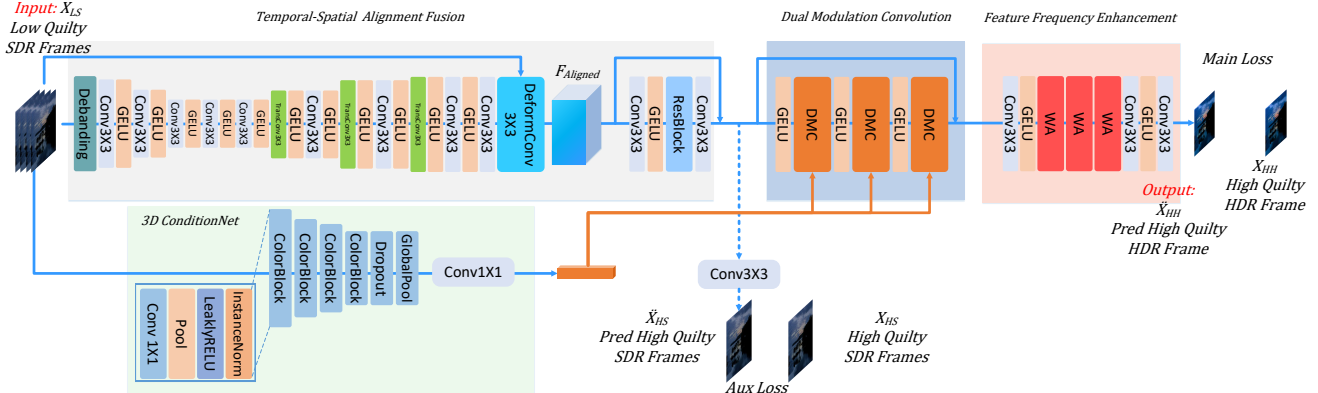


Figure 3. Framework overview. The proposed DIDNet learning de-artifacts and inverse tone mapping via two supervision. The designed temporal-spatial alignment can align feature to remove artifacts. The designed DMC and WA modules can effectively complete inverse tone mapping and enhance HDRTV quality.

through a single model is challenging due to the coupling of the two degeneracies. To address this issue, we propose an auxiliary loss for SDRTV artifact recovery, which directly improves the quality of the SDRTV frames and forces the alignment fusion component to learn the quality enhancement function. This decoupled learning approach enables a single model to effectively restore both degradations. Specifically, the fused features  $F_{fusion}$  are fed into a  $3 \times 3$  convolution to generate predicted high-quality SDRTV frames  $\hat{X}_{HS}$ . The training process uses high-quality SDRTV frames  $X_{HS}$  as a supervisory signal, which encourages the temporal-spatial alignment feature to focus on learning artifact removal and enhancing the quality of the SDRTV frames.

### 3.5. Dual Modulated Convolution

### 3.5.1 Preliminary of Global Feature Modulation

To utilize the global prior extracted from the input image, previous studies [3, 8, 21] have introduced a method called Global Feature Modulation (GFM), which has shown to be effective in tasks such as photo retouching and SDRTV-to-HDRTV conversion. GFM involves modulating the output feature of a convolutional layer using scaling and shifting operations, which can be represented by the formula (6).

$$y = \alpha \cdot \text{Conv}(x) + \beta \quad (6)$$

### 3.5.2 Feature modulation = Convolutional kernel modulation

GFM modulates the features through scaling and shifting operations using a modulation vector obtained from the condition network. However, we discovered that the same feature scaling and shifting can be achieved by modulating the convolution kernel. To demonstrate this equivalence, we

use the example of a  $1 \times 1$  convolution to deduce that modulating features is equivalent to modulating the convolution kernel. This mathematical equivalence holds true for more complex convolutions, such as the  $3 \times 3$  convolution.

To further clarify this equivalence, we consider a specific pixel convolution as an example. Without loss of generality, let us assume that the input feature channel is 3 and the output feature channel is 4. Denote the input feature as  $x \in R^3$ , the convolution kernel as  $w \in R^{4,3}$ , the output feature as  $y \in R^4$ , the modulation vector as  $\alpha \in R^4$ , and the bias as  $b \in R^4$ . The matrix dot product is represented as  $\odot$ . The convolution operation can be expanded as shown in formula (7).

In formula (7), the  $1 \times 1$  convolution is performed first. It has been proven that  $1 \times 1$  convolution is equivalent to a fully connected layer [18]. Therefore, we describe the feature modulation and convolution process as a fully connected layer. Next, the output feature is multiplied by the modulation vector  $\alpha$  and then added to the bias vector  $\beta$ . Each element in the output feature obtained after convolution interacts with the modulation vector. To simplify the process, we merge the modulation vector  $\alpha$  into the convolution kernel parameters and merge  $\beta$  into the bias parameters to obtain formula (8).

The original method of feature modulation multiplies each pixel of the image feature by a scaling factor  $\alpha$  and adds a bias term  $\beta$ . In contrast, modulating the convolution kernel achieves the same effect by modulating the kernel and bias terms directly. This approach requires significantly less computation, as the computational cost of modulating the convolution kernel is  $C_O \times C_I + C_O$ , while the cost of feature modulation is  $2 \times H \times W \times C_O$ . For the SDRTV-to-HDRTV task, which typically involves high resolutions such as 1080P and above, modulating the convolution kernel results in less than 1/1000 of the computational cost of feature modulation. Therefore, modulating the convolution

$$\begin{bmatrix} y_1 \\ y_2 \\ y_3 \\ y_4 \end{bmatrix} = \begin{bmatrix} w_{11} & w_{12} & w_{13} \\ w_{21} & w_{22} & w_{23} \\ w_{31} & w_{32} & w_{33} \\ w_{41} & w_{42} & w_{43} \end{bmatrix} \begin{bmatrix} x_1 \\ x_2 \\ x_3 \end{bmatrix} \odot \begin{bmatrix} \alpha_1 \\ \alpha_2 \\ \alpha_3 \\ \alpha_4 \end{bmatrix} + \begin{bmatrix} b_1 \\ b_2 \\ b_3 \\ b_4 \end{bmatrix} + \begin{bmatrix} \beta_1 \\ \beta_2 \\ \beta_3 \\ \beta_4 \end{bmatrix} \quad (7)$$

$$\begin{bmatrix} y_1 \\ y_2 \\ y_3 \\ y_4 \end{bmatrix} = \begin{bmatrix} w_{11} \cdot \alpha_1 & w_{12} \cdot \alpha_1 & w_{13} \cdot \alpha_1 \\ w_{21} \cdot \alpha_2 & w_{22} \cdot \alpha_2 & w_{23} \cdot \alpha_2 \\ w_{31} \cdot \alpha_3 & w_{32} \cdot \alpha_3 & w_{33} \cdot \alpha_3 \\ w_{41} \cdot \alpha_4 & w_{42} \cdot \alpha_4 & w_{43} \cdot \alpha_4 \end{bmatrix} \begin{bmatrix} x_1 \\ x_2 \\ x_3 \end{bmatrix} + \begin{bmatrix} b_1 + \beta_1 \\ b_2 + \beta_2 \\ b_3 + \beta_3 \\ b_4 + \beta_4 \end{bmatrix} \quad (8)$$

kernel provides a significant computational advantage.

### 3.5.3 Dual modulated convolution

We will further examine the modulated convolution kernel and its properties. Feature modulation involves multiplying each convolution kernel by a modulation factor. Common forms of feature modulation, such as formula (6), involve modulating features after convolution. To enhance the tone-mapping ability of our model, we designed a dual feature modulation module that modulates input features before and after convolution, as seen in formula (??). Interestingly, we found that the dual feature modulation before and after convolution can be converted to convolution kernel modulation, which we refer to as the *DMC* module. As shown in formula (9), dual feature modulation is mathematically equivalent to convolution kernel modulation, and *DMC* modulates convolution kernels of various dimensions. Ultimately, *DMC* achieves better feature transformation with significantly less computation than feature modulation.

### 3.5.4 3D ConditionNet

In order to improve the accuracy of feature modulation vector extraction and alleviate inter-frame jitter, we propose a 3D ConditionNet to extract color priors from multiple SDRTV frames. This simple yet effective design pattern results in improved HDRTV quality. The network structure

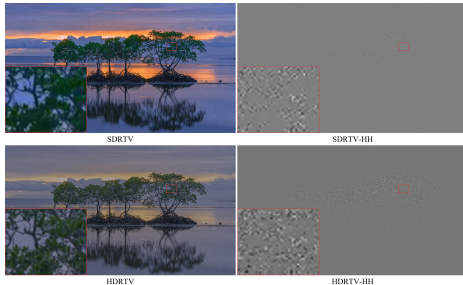


Figure 4. Comparison of high-frequency details. HDRTV has significantly more high-frequency details, as demonstrated by the wavelet transform in the HH band.

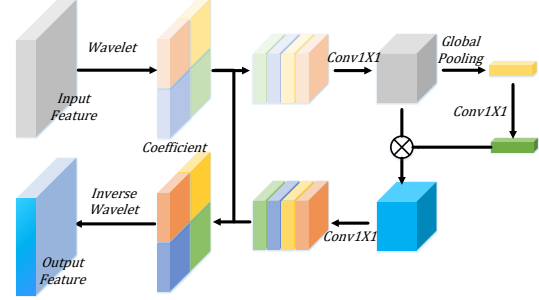


Figure 5. Wavelet Attention(WA) module.

of the 3D ConditionNet is depicted in Figure 3.

### 3.6. Wavelet attention: better restoration of high frequency detail

During our investigation, we discovered that in comparison to SDRTV, HDRTV exhibits not only differences in low-frequency information such as dynamic range and color information, but it also possesses a greater amount of high-frequency information, as illustrated in Figure 4.

To improve the quality of HDRTV, we design a wavelet attention module to enhance the high-frequency information of the features. The structure of the frequency domain attention enhancement module we design is shown in Fig.5. The specific process is as follows: first, the input feature  $x$  is decomposed into different subbands  $(ll, lh, hl, hh) \in coeffs$  by wavelet transform. Then, the different subbands are concatenated and the next one is reduced by  $1 \times 1$  convolution to obtain  $z$ . Channel attention is performed on the reduced dimensional features to obtain  $z_o$ . After a  $1 \times 1$  convolution, the features are arranged into different subbands by channel cutting, and a skip link is added. The enhanced subbands are inverted by wavelet inversion to obtain the output feature  $x_o$ .

$$\begin{aligned}
\begin{bmatrix} y_1 \\ y_2 \\ y_3 \\ y_4 \end{bmatrix} &= \begin{bmatrix} w_{11} & w_{12} & w_{13} \\ w_{21} & w_{22} & w_{23} \\ w_{31} & w_{32} & w_{33} \\ w_{41} & w_{42} & w_{43} \end{bmatrix} \begin{bmatrix} x_1 \cdot \gamma_1 \\ x_2 \cdot \gamma_2 \\ x_3 \cdot \gamma_3 \end{bmatrix} \odot \begin{bmatrix} \alpha_1 \\ \alpha_2 \\ \alpha_3 \\ \alpha_4 \end{bmatrix} + \begin{bmatrix} b_1 \\ b_2 \\ b_3 \end{bmatrix} + \begin{bmatrix} \beta_1 \\ \beta_2 \\ \beta_3 \end{bmatrix} \\
&= \begin{bmatrix} w_{11} \cdot \alpha_1 \cdot \gamma_1 & w_{12} \cdot \alpha_1 \cdot \gamma_2 & w_{13} \cdot \alpha_1 \cdot \gamma_3 \\ w_{21} \cdot \alpha_2 \cdot \gamma_1 & w_{22} \cdot \alpha_2 \cdot \gamma_2 & w_{23} \cdot \alpha_2 \cdot \gamma_3 \\ w_{31} \cdot \alpha_3 \cdot \gamma_1 & w_{32} \cdot \alpha_3 \cdot \gamma_2 & w_{33} \cdot \alpha_3 \cdot \gamma_3 \\ w_{41} \cdot \alpha_4 \cdot \gamma_1 & w_{42} \cdot \alpha_4 \cdot \gamma_2 & w_{43} \cdot \alpha_4 \cdot \gamma_3 \end{bmatrix} \begin{bmatrix} x_1 \\ x_2 \\ x_3 \end{bmatrix} + \begin{bmatrix} b_1 + \beta_1 \\ b_2 + \beta_2 \\ b_3 + \beta_3 \end{bmatrix}
\end{aligned} \tag{9}$$

$$\begin{aligned}
coeffs &= Wavelet(x) \\
z &= Conv(Concat(coeffs)) \\
s &= Conv(GlobalPooling(z)) \\
z_o &= Conv(z \cdot s) \\
coeffs_o &= UnConcat(z_o) \\
x_o &= iWavelet(coeffs_o + coeffs)
\end{aligned} \tag{10}$$

## 4. Experiment

### 4.1. Experiment setup

**Dataset.** We used the videos provided by [3] as a data set. All of these HDR videos were encoded with PQ-OETF[23] and rec.2020[33] color space, and the video resolution was 1080P. Eighteen pairs of videos were used for training and four videos were used for testing. We used X265 [20, 24] to encode the SDR videos with different fixed QP (27, 32, 37, 42) to construct datasets with different degrees of coding degradation. We perform scene segmentation on the test set and extract 348 video sequences of 10 frames each.

**Implementation details.** During the training process, we use the SDR video encoded with QP=37 as input data, and the output is high quality HDR. Our Adam optimizer [16] is used, and the initial learning rate is set to 0.0005. After 100,000 iterations, the learning rate is reduced to 1/2 of the initial rate every 60,000 iterations, and the total number of training iterations is set to 6600,000. Mean absolute error (MAE) is used to calculate the loss. In the dual loss model training, the weight of the primary loss is set to 0.8, and the weight of the auxiliary loss is set to 0.2. To verify the performance of different algorithms in a fair generalization, we take the last 6 stored weights (560000,58000,600000,620000,6400000,660000) to test the metrics. The model trained on coding degradation with a fixed QP=37 was tested on 4 different QP coding test sets. As with [10], this multiple evaluation ensures that we can accurately and fairly evaluate the performance of different models.

**Metrics.** We conducted comparative experiments on several QP-encoded test sets. And the different methods are

evaluated using seven metrics: PSNR, SSIM, MS-SSIM,  $\Delta E_{ITP}$ , VIFp [22], Harrpsi [19], and VSI [30]. These seven metrics evaluate the performance of various algorithm results in objective fidelity, structural similarity, multi-scale structural similarity, color fidelity, visual fidelity, local similarity, and visual saliency, respectively.

### 4.2. Quantitative results

We compare the proposed method with the state-of-the-art SDRTV-to-HDRTV methods (HDRTVNet[3], FMNet[27], HDCF[8], HyCondITM[21], etc.). For a fair comparison, all image quality enhancement methods were retrained in our training set, and the last 6 checkpoints of each model were selected to be tested on the test set and the average value was calculated.

**The Quantitative Results.** The quantitative results for each metric are shown in Tables 1 and 2, respectively. It can be observed that our method consistently outperforms all comparison methods in terms of mean PSNR, SSIM, MSSIM,  $\Delta E_{ITP}$ , Harrpsi, and VSI for the test set. Specifically, in the PSNR and MSSIM metrics, our method improves by 0.35 and 0.0013, respectively, compared to the previous SOTA. In terms of color difference, our method achieves a reduction of 0.614. Similar results can be found for VSI and other metrics.

### 4.3. Qualitative results

Fig.6 shows the qualitative results for the four test video frames. As can be seen, the HDRTV frames obtained from the conversion are heavily distorted by compression artifacts. The single-frame-based approach can effectively perform inverse tonal mapping of video frames, but the resulting frames are usually enhanced for noise such as coding artifacts. Our method can effectively recover the dual degradation and prevent the coding artifacts from being amplified during the inverse tone mapping process, thus improving the quality of the converted HDRTV frames.

### 4.4. Ablation study

To understand the contributions of the proposed components, we start with a baseline and gradually insert the components. The models are trained on QP=37 and the average test results over multiple QPs are reported.

Table 1. Quantitative comparison with previous methods. **Red** means best, **Green** means second, **Blue** means third. For each model on each QP, we selected the last six checkpoints for evaluation and calculated the mean of PSNR, SSIM and  $\Delta E_{ITP}$  for comparison.  $\Delta E_{ITP}$  can be used to measure the color difference, which is a key metric in the SDRTV-to-HDRTV task. The units of parameters and running time are MB and ms, respectively.

Methods	Params	Runtime	QP=27	QP=32	QP=37	QP=42	Mean-PSNR	Mean-SSIM	$\Delta E_{ITP}$
CSRNET [9]	0.006	0.8	33.598	32.472	31.288	29.946	31.826	0.9518	17.365
STDF [5]	0.889	322.1	33.978	32.810	31.591	30.163	32.135	0.9455	16.776
AILUT [29]	0.620	1.3	34.265	33.058	31.789	30.350	32.366	0.9498	16.887
AGCM [3]	0.035	2.0	34.260	33.123	31.878	30.395	32.414	0.9526	15.660
HDRTVNET [3]	1.405	102.0	34.336	33.193	31.870	30.406	32.452	0.9529	15.878
DeePSRITM [14]	2.392	753.9	34.688	33.332	31.998	30.483	32.625	0.9515	15.880
FMNet [27]	1.302	70.1	34.462	33.474	32.146	30.584	32.666	0.9523	15.183
HDRUNET [2]	1.652	265.3	34.586	33.591	32.262	30.706	32.786	0.9514	14.584
HDCFIM [8]	0.101	180.2	34.897	33.784	32.440	30.929	33.012	0.9538	15.140
HyCondITM [21]	0.605	262.4	34.860	33.862	32.573	31.103	33.100	0.9554	15.173
DIDNet	0.527	300.6	35.393	34.262	32.887	31.235	33.445	0.9563	13.970
DIDNet(Tiny)	0.386	209.4	35.061	34.040	32.702	31.123	33.232	0.9554	14.468

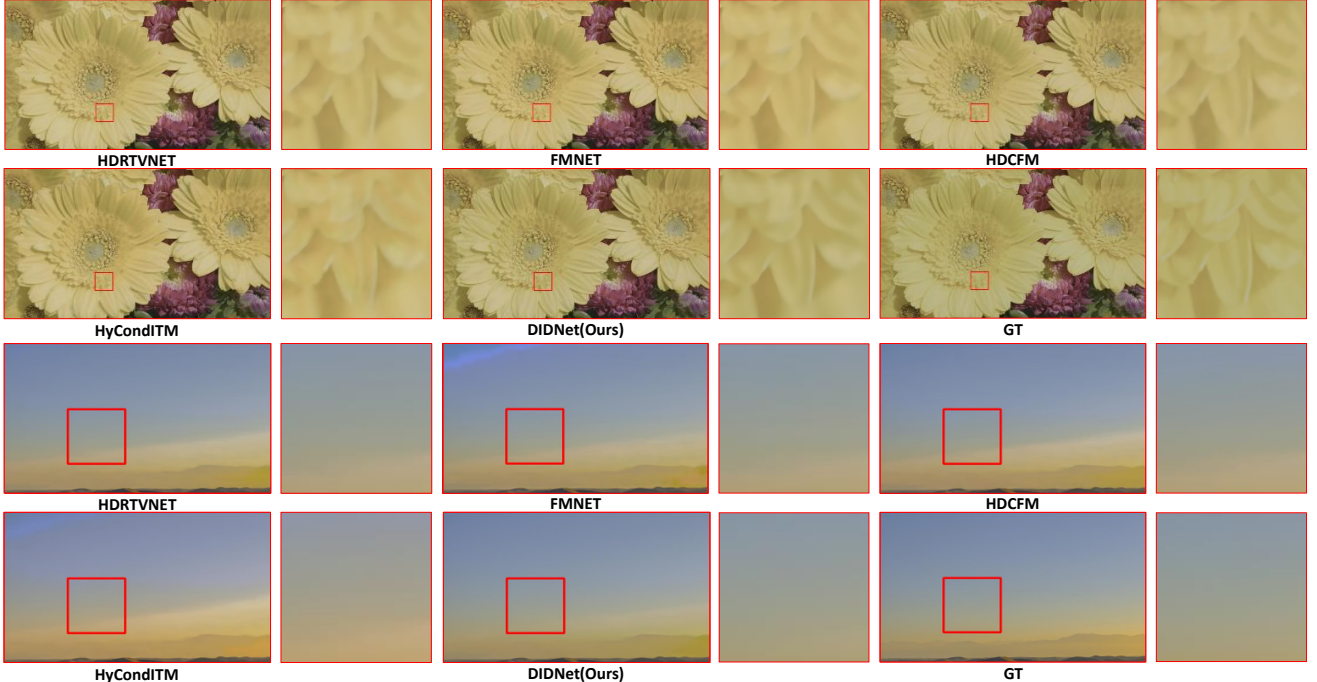


Figure 6. Qualitative results. Our proposed method produces results with fewer artifacts and higher quality than those obtained by past methods.

**Ablation of temporal-spatial alignment module.** To ablate multi-frame and temporal-spatial alignment methods, we introduce multi-frame input and alignment in multiple methods, respectively. We introduced Multi-Frame into the model design of RESNET and HDRTVNET, and the average PSNR was increased by 0.1 and 0.39, respectively. This demonstrates the effectiveness of multi-frame input. On this basis, we added a temporal-spatial alignment module on the basis of AGCM and HDRTVNET, and the PSNR

was improved by 0.08 and 0.67. It should be noted that the temporal-spatial alignment has been further improved compared to the simple multi-frame input, and the PSNR has been improved by 0.28. The PSNR improvement is summarized in Table 3 line 1-4.

**Ablation of auxiliary loss.** Since high-quality HDRTV to low-quality SDRTV is a dual degradation process, the model needs to learn both quality enhancement (artifact removal) and inverse tone mapping. A single-model learn-

Table 2. Quantitative comparison with previous methods in terms of multiscale structural similarity (MS-SSIM), visual information fidelity (VIFp), haar perceptual similarity index (Harrpsi), and visual saliency-induced index (VSI), respectively.

Methods	MS-SSIM	VIFp	Harrpsi	VSI
CSRNET [9]	0.9513	<b>0.445</b>	0.8333	0.9940
STDF [5]	0.9443	0.428	0.8260	0.9936
AILUT [29]	0.9494	0.439	0.8337	0.9938
AGCM [3]	0.9525	0.437	0.8349	0.9941
HDRTVNET [3]	0.9519	0.440	0.8400	0.9943
DeePSRITM [14]	0.9505	0.440	0.8365	0.9942
FMNet [27]	0.9516	0.441	0.8362	0.9941
HDRUNET [2]	0.9513	0.439	0.8403	0.9941
HDCFIM [8]	0.9542	0.442	<b>0.8417</b>	<b>0.9944</b>
HyCondITM [21]	<b>0.9549</b>	<b>0.446</b>	0.8412	<b>0.9944</b>
DIDNet	<b>0.9554</b>	0.443	<b>0.8433</b>	<b>0.9946</b>
DIDNet (Tiny)	<b>0.9545</b>	<b>0.444</b>	<b>0.8422</b>	<b>0.9945</b>

Table 3. Ablation study on Multi-frame input method, temporal-spatial alignment method, 3D ConditionNet, and auxiliary loss.

Method	Mean PSNR
RESNET	32.84
MF-RESNET	32.94
HDRTVNET	32.41
MF-HDRTVNET	32.80
AGCM	32.32
Temporal-Spatial Alignment + AGCM	32.40
HDRTVNET	32.41
Temporal-Spatial Alignment + HDRTVNET	33.08
Our Method W 3D ConditionNet	33.45
Our Method W/o 3D ConditionNet	33.09
Our Method W/ Aux Loss	33.45
Our Method W/o Aux Loss	33.10
Alignment + HDRUNET Aux Loss	32.93
Alignment + HDRUNET W/o Aux Loss	32.64

ing dual restoration suffers from coupled learning problems, which leads to degraded model performance. To solve this problem, we use the auxiliary loss to supervise the dual degradation learning process. We show the experimental results of introducing auxiliary loss on the PSNR metric in Table 3 line 6 in our method and Aligned-HDRUNET, respectively. After introducing the auxiliary loss in our method, the PSNR is improved by 0.35. After Aligned-HDRUNET introduces the auxiliary loss, the PSNR is improved by 0.31. The PSNR improvement is summarized in Table 3 line 6-7.

**Ablation of 3D ConditionNet.** To ablate 3D conditional network for prior extraction, we discard multi-frame input

Table 4. *DMC* and wavelet attention ablation. M1 and M2 represent Wavelet Attention *WA* and Dual Modulated Convolution *DMC* respectively.

	Baseline	M1	M2	QP=27	QP=32	QP=37	QP=42	Mean
✓				35.24	34.12	32.75	31.13	33.31
✓	✓			35.30	34.23	32.88	31.25	33.41
✓	✓	✓		35.39	34.26	32.89	31.24	33.44

Table 5. Comparison of the computational effort of global feature modulation and convolutional kernel modulation. The computation does not increase with the resolution, making this module very practical in high-resolution enhancement tasks.

Feature Shape	GFM	CKM	Ratio
720×480×64	44.22M	4.16K	0.009%
1080×1920×64	265.42M	4.16K	0.001%
2160×3840×64	1061.68M	4.16K	0.0004%

conditional network. After discarding the 3D conditional, the PSNR drops by 0.36db. It can be concluded that 3D ConditionNet can estimate the color prior more accurately, thus improving the quality of HDRTV. The PSNR improvement is summarized in Table 3 line 5.

**Ablation of wavelet attention (*WA*).** To ablate the Wavelet Attention module, we add the *WA* module on the basis of the previous module. The *WA* module enhances the features in the frequency domain, which can reconstruct more details and finer edges, and the results are shown in Table 4. The average PSNR improved from 33.31 to 33.41.

**Ablation of dual modulated convolution (*DMC*).** Our proposed modulated convolution model is significantly less computationally intensive than feature modulation. As seen in Table 5, the additional computation of modulated convolution is constant, does not increase with input image resolution, and is significantly less computationally intensive than feature modulation. We conducted ablation experiments, and *DMC* can further improve HDRTV quality. It is reported from Table 4 that after adding *DMC*, the PSNR of converted HDRTV is increased by 0.03.

## 5. Conclusion

We analyze the difficulties in the current SDRTV-o-HDRTV process, including inaccurate inverse tone mapping, amplified artifacts, difficulties in learning the coupling, and insufficient high-frequency information. The corresponding modules Dual Modulated Convolution (*DMC*), Auxiliary Loss, and Wavelet Attention (*WA*) are proposed. *DMC* can perform inverse tone mapping more accurately. The Proposed auxiliary loss can decouple the learning process of inverse tone mapping and artifact repair, and obtain high-quality HDRTV content. *WA* enhances the features in the frequency domain, which can further improve the

quality of HDRTV. Our proposed method makes SDRTV-to-HDRTV practical, solves the issue of low visual quality caused by the amplification of artifacts, and can convert real-world low quality SDRTV into high-quality HDRTV.

## References

- [1] Anders BallestadAndrey and KostinGregory John WARD. Method and apparatus for image data transformation, U.S. Patent US9224363B2, 2015.
- [2] Xiangyu Chen, Yihao Liu, Zhengwen Zhang, Yu Qiao, and Chao Dong. Hdrunet: Single image hdr reconstruction with denoising and dequantization. In *Proceedings of the IEEE/CVF Conference on Computer Vision and Pattern Recognition*, pages 354–363, 2021.
- [3] Xiangyu Chen, Zhengwen Zhang, Jimmy S. Ren, Lynhoo Tian, Yu Qiao, and Chao Dong. A new journey from sdrtv to hdrtv. In *Proceedings of the IEEE/CVF International Conference on Computer Vision (ICCV)*, pages 4500–4509, October 2021.
- [4] Jifeng Dai, Haozhi Qi, Yuwen Xiong, Yi Li, Guodong Zhang, Han Hu, and Yichen Wei. Deformable convolutional networks. In *Proceedings of the IEEE international conference on computer vision*, pages 764–773, 2017.
- [5] Jianing Deng, Li Wang, Shiliang Pu, and Cheng Zhuo. Spatio-temporal deformable convolution for compressed video quality enhancement. In *Proceedings of the AAAI conference on artificial intelligence*, volume 34, pages 10696–10703, 2020.
- [6] Jun Gong, Siyuan Li, Shiyu Chen, Liang Nie, Xin Cheng, Zhiqiang Zhang, and Wenxin Yu. Image inpainting based on interactive separation network and progressive reconstruction algorithm. *IEEE Access*, 10:67814–67825, 2022.
- [7] Gang He, Shan Wu, Simin Pei, Li Xu, Chang Wu, Kepeng Xu, and Yunsong Li. Fm-vsrl: Feature multiplexing video super-resolution for compressed video. *IEEE Access*, 9:88060–88068, 2021.
- [8] Gang He, Kepeng Xu, Li Xu, Chang Wu, Ming Sun, Xing Wen, and Yu-Wing Tai. Sdrtv-to-hdrtv via hierarchical dynamic context feature mapping. In *Proceedings of the 30th ACM International Conference on Multimedia, MM '22*, page 2890–2898, New York, NY, USA, 2022. Association for Computing Machinery.
- [9] Jingwen He, Yihao Liu, Yu Qiao, and Chao Dong. Conditional sequential modulation for efficient global image retouching. In *European Conference on Computer Vision*, pages 679–695. Springer, 2020.
- [10] Man M. Ho, Jinjia Zhou, and Gang He. Rr-dncnn v2.0: Enhanced restoration-reconstruction deep neural network for down-sampling-based video coding. *IEEE Transactions on Image Processing*, 30:1702–1715, 2021.
- [11] Yanting Hu, Jie Li, Yuanfei Huang, and Xinbo Gao. Channel-wise and spatial feature modulation network for single image super-resolution. *IEEE Transactions on Circuits and Systems for Video Technology*, 30(11):3911–3927, 2019.
- [12] Wonjong Jang, Gwangjin Ju, Yucheol Jung, Jiaolong Yang, Xin Tong, and Seungyong Lee. Stylecarigan: caricature generation via stylegan feature map modulation. *ACM Transactions on Graphics (TOG)*, 40(4):1–16, 2021.
- [13] Soo Ye Kim, Jihyong Oh, and Munchurl Kim. Deep sr-itm: Joint learning of super-resolution and inverse tone-mapping for 4k uhd hdr applications. In *international conference on computer vision*, 2019.
- [14] Soo Ye Kim, Jihyong Oh, and Munchurl Kim. Deep sr-itm: Joint learning of super-resolution and inverse tone-mapping for 4k uhd hdr applications. In *Proceedings of the IEEE/CVF International Conference on Computer Vision*, pages 3116–3125, 2019.
- [15] Soo Ye Kim, Jihyong Oh, and Munchurl Kim. Jsi-gan: Gan-based joint super-resolution and inverse tone-mapping with pixel-wise task-specific filters for uhd hdr video. *national conference on artificial intelligence*, 2019.
- [16] Diederik P Kingma and Jimmy Ba. Adam: A method for stochastic optimization. *arXiv preprint arXiv:1412.6980*, 2014.
- [17] Siyuan Li, Lu Lu, Zhiqiang Zhang, Xin Cheng, Kepeng Xu, Wenxin Yu, Gang He, Jinjia Zhou, and Zhuo Yang. Interactive separation network for image inpainting. In *2020 IEEE International Conference on Image Processing (ICIP)*, pages 1008–1012, 2020.
- [18] Min Lin, Qiang Chen, and Shuicheng Yan. Network in network. *CoRR*, abs/1312.4400, 2013.
- [19] Rafael Reisenhofer, Sebastian Bosse, Gitta Kutyniok, and Thomas Wiegand. A haar wavelet-based perceptual similarity index for image quality assessment. *Signal Processing: Image Communication*, 61:33–43, 2018.
- [20] Heiko Schwarz, Detlev Marpe, and Thomas Wiegand. Overview of the scalable video coding extension of the h.264/avc standard. *IEEE Transactions on circuits and systems for video technology*, 17(9):1103–1120, 2007.
- [21] Tong Shao, Deming Zhai, Junjun Jiang, and Xianming Liu. Hybrid conditional deep inverse tone mapping. In *Proceedings of the 30th ACM International Conference on Multimedia, MM '22*, page 1016–1024, New York, NY, USA, 2022. Association for Computing Machinery.
- [22] Hamid R Sheikh and Alan C Bovik. A visual information fidelity approach to video quality assessment. In *The first international workshop on video processing and quality metrics for consumer electronics*, volume 7, pages 2117–2128. sn, 2005.
- [23] SMPTE Standard. High dynamic range electro-optical transfer function of mastering reference displays. *SMPTE ST*, 2084(2014):11, 2014.
- [24] Gary J. Sullivan, Jens-Rainer Ohm, Woo-Jin Han, and Thomas Wiegand. Overview of the high efficiency video coding (hevc) standard. *IEEE Transactions on Circuits and Systems for Video Technology*, 22(12):1649–1668, 2012.
- [25] Xiantao Wang, Kelvin CK Chan, Ke Yu, Chao Dong, and Chen Change Loy. Edvr: Video restoration with enhanced deformable convolutional networks. In *Proceedings of the IEEE/CVF Conference on Computer Vision and Pattern Recognition Workshops*, pages 0–0, 2019.

- [26] Bing Xu, Junfei Zhang, Rui Wang, Kun Xu, Yong-Liang Yang, Chuan Li, and Rui Tang. Adversarial monte carlo denoising with conditioned auxiliary feature modulation. *ACM Trans. Graph.*, 38(6):224–1, 2019.
- [27] Gang Xu, Qibin Hou, Le Zhang, and Ming-Ming Cheng. Fmnet: Frequency-aware modulation network for sdr-to-hdr translation. In *Proceedings of the 30th ACM International Conference on Multimedia, MM ’22*, page 6425–6435, New York, NY, USA, 2022. Association for Computing Machinery.
- [28] Ning Xu, Tao Chen, James E. Crenshaw, Timo Kunkel, and Bongsun Lee. Methods and systems for inverse tone mapping, U.S. Patent US9607364B2, 2013.
- [29] Canqian Yang, Meiguang Jin, Xu Jia, Yi Xu, and Ying Chen. Adaint: Learning adaptive intervals for 3d lookup tables on real-time image enhancement. In *Proceedings of the IEEE/CVF Conference on Computer Vision and Pattern Recognition*, pages 17522–17531, 2022.
- [30] Lin Zhang, Ying Shen, and Hongyu Li. Vsi: A visual saliency-induced index for perceptual image quality assessment. *IEEE Transactions on Image Processing*, 23(10):4270–4281, 2014.
- [31] Zhiqiang Zhang, Wenxin Yu, Jinjia Zhou, Xuewen Zhang, Ning Jiang, Gang He, and Zhuo Yang. Customizable gan: A method for image synthesis of human controllable. *IEEE Access*, 8:108004–108017, 2020.
- [32] Zhiqiang Zhang, Jinjia Zhou, Wenxin Yu, and Ning Jiang. Text-to-image synthesis: Starting composite from the foreground content. *Information Sciences*, 607:1265–1285, 2022.
- [33] Ruidong Zhu, Zhenyue Luo, Haiwei Chen, Yajie Dong, and Shin-Tson Wu. Realizing rec. 2020 color gamut with quantum dot displays. *Optics express*, 23(18):23680–23693, 2015.
- [34] Xizhou Zhu, Han Hu, Stephen Lin, and Jifeng Dai. Deformable convnets v2: More deformable, better results. In *Proceedings of the IEEE/CVF conference on computer vision and pattern recognition*, pages 9308–9316, 2019.
- [35] Wangmeng Zuo, Kai Zhang, and Lei Zhang. *Convolutional Neural Networks for Image Denoising and Restoration*, pages 93–123. Springer International Publishing, Cham, 2018.